ELSEVIER

Chemical Engineering Journal 72 (1999) 79–82

Chemical Engineering Journal

Short communication

On the magnetohydrodynamics of natural convective diffusion boundary layers in coupled horizontal electric and magnetic fields

Thomas Z. Fahidy*

Department of Chemical Engineering, University of Waterloo, Waterloo, Ont., Canada N2L 3G1

Received 3 July 1998; received in revised form 2 October 1998; accepted 21 October 1998

Abstract

An approximate method for the estimation of the mean velocity and the root mean square velocity in the natural-convective diffusion boundary layer under the influence of weak magnetic fields is presented. The method applies to vertical solid surfaces when the electric and magnetic field are horizontal and mutually transverse; the magnetic field may support or oppose the gravity field. Extension to axisymmetric surfaces is feasible by appropriate modifications of the constitutive equations.

Keywords: Natural convection; Vertical surface; Magnetic field; Velocity; Diffusion boundary layer

1. Introduction

Due to the mathematical complexity of the governing equations of the diffusion boundary layers existing in externally imposed magnetic fields, the lack of a general/analytical solution of their velocity field has been pointed out in both earlier e.g. [1,2] and recent e.g. [3,4] literature. In the specific case of natural convection at vertical solid surfaces, an approximate method to describe the concentration field in horizontally transverse electric and magnetic fields under electrolytic mass transport control has been discussed [2,5], but without a thorough analysis of the hydrodynamics of the boundary layer. The purpose of the current communication is to present an approximate method for the estimation of velocity components and the RMS velocity in such configurations. The approach can equally be applied to gravity-supporting and gravity-opposing magnetohydrodynamic (MHD) body force action in the presence of weak magnetic fields.

2. Problem formulation

Fig. 1 illustrates two such configurations in a liquid medium with a vertical solid surface. The direction of the MHD force is determined by the direction of the current when the direction of the imposed magnetic flux density is fixed. Depending on the direction of the current, the MHD body force with density magnitude $j_y B_z$ either supports (configuration *a*) or opposes (configuration *b*) the gravity force; hence the magnetic field effect on natural convection will be different in the two cases. Following the classical theory of natural convection by Levich [6], the dominant velocity components in the boundary layer may be written as

$$v_x = 4\nu\left(\frac{g\alpha}{4\nu^2}\right)^{1/2} x^{1/2}\,\frac{\mathrm{d}f}{\mathrm{d}\eta} \tag{1a}$$

$$v_y = \nu\left(\frac{g\alpha}{4\nu^2}\right)^{1/4}\{(\eta[\mathrm{d}f/\mathrm{d}\eta] - 3f)/x^{1/4}\} \tag{1b}$$

where

$$f(\eta) = \frac{\beta\eta^2}{2} - \frac{\eta^3}{6} + 0.037158(\beta\mathrm{Sc})^{1/3}\eta^4 \tag{2}$$

and

$$\eta \equiv \frac{(g\alpha/4\nu^2)^{1/4} y}{x^{1/4}} \tag{3}$$

is a similarity transformation variable. The parameter β is related to the magnetic flux density [2] by the expression

$$\beta = \frac{1.092(1/3 + j_y B_z/2g\rho\alpha)^{3/4}}{\mathrm{Sc}^{1/4}} \tag{4}$$

*Corresponding author. Fax: +1-519746-4979; e-mail: t-fahidy@engmail.uwaterloo.ca

1385-8947/99/$ – see front matter
PII: S1385-8947(98)00142-9

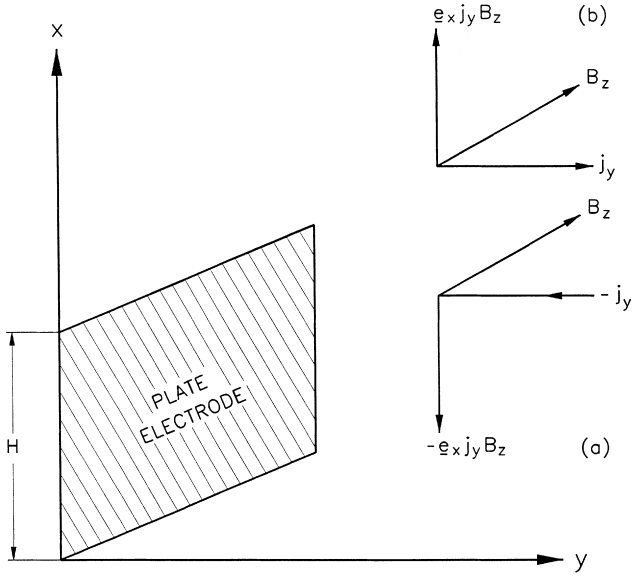

Fig. 1. Electrode geometry and electric/magnetic field configuration.

which is a modification of the magnetic field-free relationship [[6], Eqs. 23.27, p. 133]. The dimensionless mass transport rate is equally modified to account for the magnetic field effect as

$$\mathrm{Sh} = 0.886\left(\frac{1}{3} + \frac{j_y B_z}{2g\rho\alpha}\right)^{1/4} \mathrm{Ra}^{1/4} \tag{5}$$

It is important to note that in configuration *a*, where the gravity force is supported by the magnetic field, the second term in the brackets of Eqs. (4) and (5) has a negative sign. Eq. (5) carries an implicit relationship between the diffusion limiting current density and the magnetic flux density (see Section 4).

While Eqs. (1a) and (1b) permits, in principle, the mapping of the velocity profile at any arbitrary position inside the boundary layer, a quicker and more amenable measure of the MHD behaviour is offered by the mean values of the velocity components, and by the RMS velocity. These quantities are defined as

$$\bar{v}_x = \left[\frac{1}{H\delta}\right] \int_0^{\delta}\int_0^{H} v_x \,\mathrm{d}x\,\mathrm{d}y \tag{6}$$

$$\bar{v}_y = \left[\frac{1}{H\delta}\right] \int_0^{\delta}\int_0^{H} v_y \,\mathrm{d}x\,\mathrm{d}y \tag{7}$$

and

$$v_{\mathrm{RMS}} = \left\{ \left[\frac{1}{H\delta}\right] \int_0^{\delta}\int_0^{H} (v_x^2 + v_y^2)\,\mathrm{d}x\,\mathrm{d}y \right\}^{1/2} \tag{8}$$

Some difficulty arises in conjunction with Eq. (7) due to the theoretically infinitely large value of v_y at the bottom edge of the vertical plate (Eq. (1b)), which can, however, be circumvented by integrating along the *x*-axis from an appropriately chosen small value of $x = a$, instead of the rigorous lower limit of zero. This procedure is demonstrated in Section 4.

3. Problem solution

Upon rather cumbersome algebraic manipulations, Eqs. (6) and (7) may be solved as

$$\bar{v}_x = 0.4A_1A_3\beta H^{1/4}\delta - 0.1667A_1A_3^2\delta^2 + 0.3333A_1A_2A_3^3H^{-1/4}\delta^3 \tag{9}$$

$$\bar{v}_y = -0.667A_3^2\,\nu\beta H^{-3/4}\delta^2 + 0.005567\nu\beta^{1/3}\mathrm{Sc}^{1/3}A_3^5H^{-1}\delta^4[H^{-1/4} - \lim_{x\to a} x^{-1/4}] \tag{10}$$

and the RMS velocity is obtained as

$$v_{\mathrm{RMS}} = \{A_4\gamma_1 + A_5^2\gamma_2 + A_6^2\gamma_3 + 2A_4(A_5 + A_6)\gamma_4 + 2A_5A_6\gamma_5 + A_7^2\gamma_6 + 2A_7A_8\gamma_7 + A_8^2\gamma_8\}^{1/2} \tag{11}$$

The lumped parameters appearing in Eqs. (9)–(11) are listed in Table 1.

4. Numerical illustration

The computation procedure is illustrated by considering the electrolytic deposition of nickel from an aqueous nickel chloride/boric acid solution used in electroplating practice. Pertinent parameters of the experimental cell using a parallel-plate copper cathode and a nickel anode [7] are shown in Table 2. The experimental cell closely mimics (except for

Table 1
Lumped parameters in the evaluation of the mean velocity quantities in the natural *B* convective diffusion boundary layer

A_1	$4\nu[g\alpha/4\nu^2]^{1/2}$
A_2	$0.1486\beta^{1/3}\ \mathrm{Sc}^{1/3}$
A_3	$[g\alpha/4\nu^2]^{1/4}$
A_4	$A_1\ A_3\ \beta$
A_5	$-0.5A_1{A_3}^2$
A_6	$A_1\ A_2\ {A_3}^3$
A_7	$-0.5\nu{A_3}^3\ \beta$
A_8	$0.006958\nu\beta^{1/3}\ \mathrm{Sc}^{1/3}\ {A_3}^5$
γ_1	$0.2222H^{1/2}\ \delta^2$
γ_2	$0.2\delta^4$
γ_3	$0.2857H^{-1/2}\ \delta^6$
γ_4	$0.2H^{1/4}\delta^3$
γ_5	$0.2222H^{-1/4}\delta^5$
γ_6	$-0.4H^{-3/2}\ \delta^4$
γ_7	$-0.1428H^{-2}\ \delta^6$
γ_8	$-0.07407H^{-5/2}\ \delta^8$

Note: The terms (i, $i = 1, \ldots, 8$ were obtained by double integration on [0, H] in the *x*-direction and on [0, δ] in the *y*-direction.

Table 2
Parameters of an experimental electrolytic nickel deposition process [7] in Section 4. The height of the vertical cathode plate is 1 cm; its effective area is 1.25 cm^2

Quantity and unit	Numerical value	Reference
Concentration of $NiCl_2$ (mol dm^{-3})	1.0	[8]
Concentration of H_3BO_3 (mol dm^{-3})	0.485	[8]
Bulk solution density (kg dm^{-3})	1.1134	[9]
Bulk solution viscosity (Pa s)	8.903×10^{-4}	[10]
Bulk solution diffusivity ($m^2 s^{-1}$)	1.091×10^{-9}	[10]
Bulk solution pH	0.9–1.1	[8]
Cathode efficiency (%)	90–100	[8]
Electrolyte diffusivity ($m^2 s^{-1}$)	1.091×10^{-9}	[10]
Kinematic viscosity ($m^2 s^{-1}$)	1.23×10^{-6}	C
Densification coefficient	0.105	C
Schmidt number Sc	1127	C
Grashof number Gr	6.78×10^5	C
Rayleigh number Ra = ScGr	7.64×10^8	C

Note: The symbol 'C' denotes a calculated value.

size) an industrial process [8]. Since the cathode efficiency range is normally between 90% and 100%, the computed results are based on limiting diffusion currents calculated directly from Eq. (5) at a 100% cathode efficiency in order to avoid the guessing of the fraction of current expended on hydrogen evolution (if the true cathode efficiency ε_{cath} is known, the numerical results are readily adjusted by taking $\varepsilon_{cath} j_y$ instead of j_y).

4.1. Mean velocity components

Eqs. (9) and (10) yield, respectively,

$$\bar{v}_x = 0.0169\beta + 9.532 \times 10^{-4}\beta^{1/3} - 1.474 \times 10^{-3} \ (\mathrm{m\,s^{-1}}) \tag{12}$$

and

$$10^7\,\bar{v}_y = -47.76\beta + 2.28\beta^{1/3}(1 - \lim_{x\to a} x^{-1/4}) \ (\mathrm{m\,s^{-1}}) \tag{13}$$

As shown in Table 3, the average velocity component normal to the vertical surface remains negligible in the gravity-supporting case even at $a = 10^{-10}$ m (approximate thickness of the Helmholtz double layer). At $a = 10^{-12}$ m even the largest value ($10^7\ v_y = -3.17$ at $B_z = 0$) is only about 10% of the magnitude of the vertical mean velocity component. In the gravity-opposing case (Table 3) similar observations can be made.

4.2. The root mean square velocity

Numerical evaluation of Eq. (11) yields the relationship

$$10^2 v_{RMS} = \left\{0.0391 - 0.749\beta + 3.9813\beta^2 - 0.0562\beta^{1/3} + 0.0234\beta^{2/3} + 0.484\beta^{4/3}\right\}^{1/2} (\mathrm{ms^{-1}}) \tag{14}$$

Table 3
Hydrodynamic characteristics of the diffusion boundary layer in the numerical illustration.(a) gravity force supported by the magnetic field

B_z (T)	j_y (A m^{-2})	β	$10^4\ v_x$ ($m\,s^{-1}$)	$10^7\ v_y$ ($m\,s^{-1}$)	$10^4\ v_{RMS}$ ($m\,s^{-1}$)
Gravity force supported by the magnetic field					
0	2356	0.0827	3.41	−102.3	4.37
0.05	2263	0.0733	1.66	−97.9	3.26
0.067	2232	0.0702	1.08	−96.5	3.17
0.075	2216	0.0687	0.80	−95.7	3.14
0.100	2167	0.0643	−0.36	−93.5	3.38
Gravity force opposed by the magnetic field					
0	2356	0.0827	3.41	−102.3	4.37
0.05	2446	0.0925	5.22	−106.5	5.96
0.067	2475	0.0958	5.84	−107.8	6.59
0.100	2532	0.1026	7.08	−110.5	7.92

with illustrative values shown in Table 3. Reversal in the numerical values of the sixth column in case (a) is caused by restrictions of the model equations to weak magnetic fields [2]. A careful search for the reversal point indicates that v_{RMS} reaches its lowest value of $\cong 0.0315$ cm s^{-1} at $B_z \cong 75$ mT, which represents the upper bound of the model validity range.

5. Discussion

As discussed earlier, the estimation procedure involving Eqs. (4) and (5) is a first-order approximation limited to weak magnetic fields. A second-order approximation, valid for a wider range of the magnetic flux density, requires the computation of incomplete gamma functions and a cumbersome multiple successive iteration scheme to calculate the parameter β [2]. Since the underlying principles of the second-order approximation are not different from the first-order approximation, it is not treated here.

The composition of the electrolyte in Section 4 indicates a supporting electrolyte to total electrolyte ratio 'r' [11] less than unity, implying a limiting current to diffusion limiting current ratio larger than unity. From current ratio versus $r^{1/2}$ data available in the literature [11,12] this current ratio is estimated to be about 1.15, indicating a rather small effect on the numerical values of the hydrodynamic parameters.

From a fully rigorous point of view, the magnetic field effect would also be manifest by the existence of an MHD boundary layer, in addition to the diffusion boundary layer. In the experimental cell of Section 4, the numerical value of 22 cm computed for the MHD boundary layer thickness at $B = 50$ mT, compared to the diffusion boundary layer thickness estimated [6] at about 0.01 cm at $B = 50$ mT, shows that the MHD boundary layer is totally unimportant (at lower values of B the thickness of the MHD boundary layer is larger). An alternative argument in terms of the dimensionless Hartmann number Ha of classical MHD theory e.g. [13] leads to the same conclusion, inasmuch as the estimated

values of Ha are smaller than unity; for the MHD boundary layer to possess an important role, the Ha $\gg 1$ condition must be satisfied.

Finally, inspection of Table 3 indicates the dominance of the vertical velocity component over the diffusion boundary layer region. However, very high *local* values of the normal velocity component can be expected close to the vertical surface near its lower edge. The relative importance of the magnetic field strength becomes minimal at such locations, since $v_y \rightarrow \infty$ when x approaches zero, regardless of the magnetic field effect on $f(\eta)$.

The method described here can be extended to other (at least axisymmetric) natural convective surfaces with geometrically appropriate modifications of the constitutive equations of Section 2[14]. The topic is beyond the scope of this paper.

Acknowledgements

The author's work in the area of magnetic field effects on electrolyte behaviour has been supported by the Natural Sciences and Engineering Research Council of Canada (NSERC).

Appendix

Nomenclature

a	a small distance measured vertically upwards from the bottom edge of the solid surface (cm)
B_z	magnitude of the imposed magnetic flux density (T)
C	bulk electrolyte concentration (mol m^{-3})
D	electrolyte diffusivity (m^2 s^{-1})
F	Faraday's number (96487 C mol^{-1})
$f(\eta)$	similarity transformation function of dimensionless variable η
g	acceleration due to gravity (m s^{-2})
H	height of the solid surface (m)
Ha	Hartmann number (–) $B_z(H/2)(\sigma/\nu\rho)^{0.5}$
j_y	magnitude of the imposed current density (A m^{-2})
n	valency (−)
Ra	Rayleigh number (–) $g\alpha H^3/\nu D$
Sc	Schmidt number (–) ν/D
Sh	Sherwood number (–) $j_y H/nFDC$
v_x	vertical velocity component in the diffusion boundary layer (m s^{-1}); v_x its mean value
v_y	normal velocity component in the diffusion boundary layer (m s^{-1}); v_y its mean value
v_{RMS}	root mean square velocity in the diffusion boundary layer (m s^{-1})
x	vertical coordinate (m)
y	normal coordinate (m)
α	densification coefficient (–)
β	boundary layer parameter (–)
δ	boundary layer thickness (m)
η	similarity transformation variable (–)
ν	kinematic viscosity (m^2 s^{-1})
ρ	density (kg m^{-3})
σ	electrolyte conductivity (S m^{-1})

Superscript

–	mean value averaged over the diffusion boundary layer

References

[1] T.Z. Fahidy, J. Appl. Electrochem. 13 (1983) 553.
[2] T.Z. Fahidy, Chem. Eng. J. 7 (1974) 21.
[3] G.B. Ngo Boum, Etude Numerique du Transport de Matiere au Sein d'un Electrolyte: Effet d'un Champ Magnetique, Doctoral dissertation, Institut National Polytechnique de Grenoble, 1998.
[4] N. Leventis, M. Chen, X. Gao, M. Canalas, P. Zhang, J. Phys. Chem. B 102 (1998) 3512.
[5] T.Z. Fahidy, Chem. Eng. J. 17 (1979) 245.
[6] V.I. Levich, Physicochemical Hydrodynamics, Prentice Hall, Englewood Cliffs, NJ, 1962.
[7] F. Boreyri, K. Pham, M. Vilela, Effect of Magnetic Field on the Electrodeposition of Nickel, final year undergraduate research project, Department of Chemical Engineering, University of Waterloo, Canada, 1998.
[8] H.J. Durney, Electroplating Engineering Handbook, 4th ed., Table 19, Van Nostrand Reinhold, New York, 1984, p. 250.
[9] V.M.M. Lobo, J.L. Quresma, Phys. Sci. Data 41, Handbook of Electrolyte Solutions Part B, Elsevier, New York 1989.
[10] R.H. Stokes, S. Phang, R. Mills, J. Sol. Chem. 8 (1979) 489.
[11] J.S. Newman, Intern. J. Heat Mass Transfer 10 (1967) 883.
[12] J.S. Newman, Electrochemical Systems, 2nd ed., Chap. 19, Prentice Hall, Englewood Cliffs, NJ, 1991.
[13] J.A.Shercliff, A Textbook of Magnetohydrodynamics, Pergamon Press, Oxford, 1965.
[14] T.Z. Fahidy, Principles of Electrochemical Reactor Analysis, Section 7.4, Elsevier, Amsterdam, 1985.